Supporting Information for "Seasonal strength of terrestrial net ecosystem CO_2 exchange from North America is underestimated in global inverse modeling"

Yu Yan Cui[1], Li Zhang[1], Andrew R. Jacobson[2,3], Matthew S. Johnson[4], Sajeev Philip[5], David Baker[6], Frederic Chevallier[7], Andrew E. Schuh[6], Junjie Liu[8], Sean Crowell[9], Hélène E. Peiro[9], Feng Deng[10], Sourish Basu[11], and Kenneth J Davis[1,12]

[1]Department of Meteorology and Atmospheric Science, The Pennsylvania State University, University Park, PA, USA

[2]Cooperative Institute for Research in Environmental Sciences, University of Colorado, Boulder, CO, USA

[3]NOAA Earth System Research Laboratory, Global Monitoring Laboratory, Boulder, CO, USA

[4]Earth Science Division, NASA Ames Research Center, Moffett Field, CA, USA

[5]Universities Space Research Association, NASA Ames Research Center, Mountain View, CA, USA

[6]Cooperative Institute for Research in the Atmosphere, Colorado State University, Fort Collins, CO, USA

[7]Laboratoire des Sciences du Climat et de L'Environnement, LSCE/IPSL, CEA-CNRS-UVSQ, Université Paris-Saclay, Gif-sur-Yvette, France

[8]Jet Propulsion Laboratory, California Institute of Technology, Pasadena, CA, USA

[9]University of Oklahoma, School of Meteorology, Norman, OK, USA

[10]Department of Physics, University of Toronto, Toronto, ON, Canada

[11]NASA GSFC GMAO / University of Maryland, Goddard Space Flight Center, Greenbelt, MD, USA

[12]Earth and Environmental Systems Institute, The Pennsylvania State University, University Park, PA, USA

Contents of this file

1. Text S1
2. Figures S1 to S7
3. Tables S1 to S2

Text S1.

The background CO_2 mole fractions (C_{bkg}) for each receptor are determined by combining the sensitivity of each receptor to the initial condition (m, prior to the backward 10 days) and the OCO-2 v9 MIP global optimized CO_2 mole fraction fields (C_{CO_2}) (Equation S1).An example of the background determination is shown in Figure S1.

$$C_{bkg} = m \cdot C_{CO_2} \tag{1}$$

where m is the spatially and temporally resolved sensitivity field of the receptors to the initial conditions (dimension: n × i × j × z, n denotes the receptors, i, j, and z are latitude, longitude, and altitude, respectively), C_{CO_2} is the corresponding inversion-optimized CO_2 mole fraction fields (dimension: i × j × z), and C_{bkg} is the determined background values for each receptor (dimension: n × 1).

We define 12 ecoregions in the study (Figure S2) and calculated the influence functions with these ecoregions. For each receptor, the ecoregion associated with the largest contribution to the influence functions is tagged as the representative region (Figure S2).

We calculate the seasonal NEE flux budget (PgC/yr) for the shaded areas (Figure S3) and analyze the relationships between the regional flux strength and the estimates of Mean Bias Error based on the ACT-America aircraft campaigns.

The maps of averaged CO_2 NEE during the ACT-America campaign months from the inversion products are shown in Figure S4, Figure S5,Figure S6, and Figure S7.

As mentioned in the main text, a suite of gridded global CO_2 NEE products at 3-hourly resolution from nine members of OCO-2 v9 MIP (Table S1) was created for the four ACT-America Campaign periods (summer 2016, winter 2017, fall 2017, and spring 2018).

The global atmospheric CO_2 inversion models are driven by different prior flux components including Fossil fuel, NEE, fire and ocean fluxes. All models used the same fossil fuel flux products from ODIAC 2018 version (`https://gmao.gsfc.nasa.gov/gmaoftp/sourish/ODIAC/2018/distrib/`), and the prior flux from NEE, fire, and ocean components are listed in Table S2.

Table S1. Basic information of the nine global inversion systems evaluated in the study.

Inversion system	Transport model	Met driver	Inversion method	Flux spatial resolution	Flux temporal resolution
CT	TM5	ERA-Interim	EnKF	1x1	3-hourly
OU	TM5	ERA-Interim	4DVar	1x1	3-hourly
TM5-4DVAR	TM5	ERA-Interim	4DVar	2x3	3-hourly
Ames	GEOS-Chem	MERRA-2	4DVar	4x5	3-hourly
CMS-Flux	GEOS-Chem	MERRA-2	4Dvar	4x5	3-hourly
CSU	GEOS-Chem	GEOS-FP	Beyesian synthesis	1x1	3-hourly
UT	GEOS-Chem	GEOS-FP	4Dvar	4x5	3-hourly
Baker-mean	PCTM	MERRA-2	4Dvar	2x2.5	3-hourly
CAMS	LMDZ3	ERA5	Variational	1.875 x 3.75	3-hourly

Table S2. Prior inventories of CO_2 flux components

	NEE	Ocean	Fire
CT	CT2019 CASA-GFED4	CT2019 OI	CT2019 w4 (based on GFED4)
OU	CASA-GFED3	Takahashi	GFED3
TM5-4DVAR	SiB4	Lofi	GFED4
Ames	CT2019 CASA-GFED4	CT2019 OI	CT2019 w4 (based on GFED4)
CMS-Flux	CARDAMOME	ECCO-Darwin	GFED3
CSU	SIB4/MERRA	CT2015 OI	GFED4-HEMCO
UT	CASA-GFED4	Takahashi	GFED4
Baker-Mean	CASA-GFED4	Takahashi	GFED3
CAMS	ORCHIDEE	CMEMS	GFED4

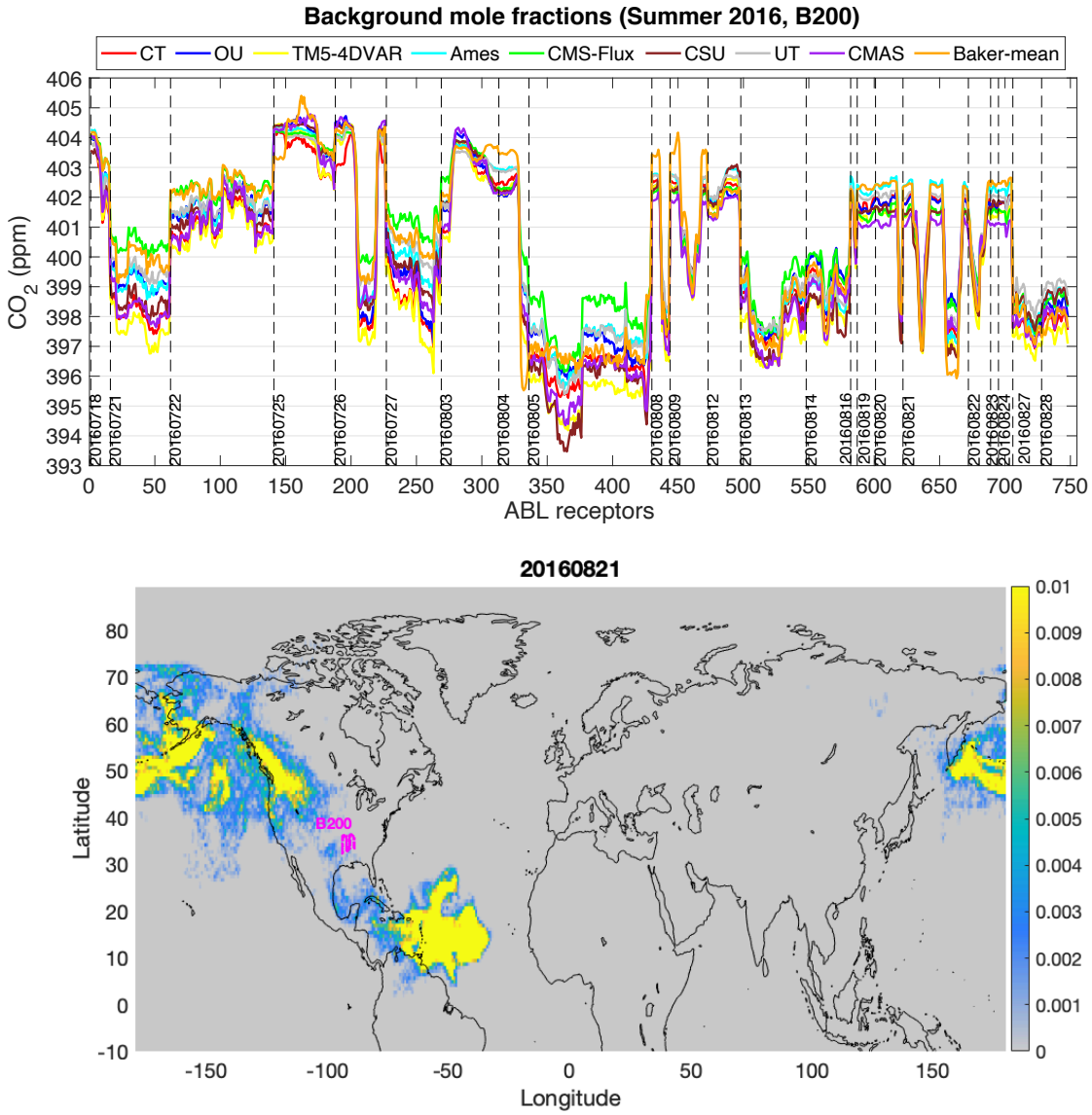

Figure S1. The upper panel shows the background CO2 mole fractions for each receptor from the all B200 flights during the ACT summer 2016 campaign for each OCO-2 v9 MIP model that is associated with the IS experiment. The lower panel shows the integrated sensitivity of all receptors from one single B200 flight (pink line is the flight track) to the initial condition (backward 10 days) across all vertical layers. Background CO_2 (C_{bkg}) for all ACT airborne ABL observations were computed in this fashion.

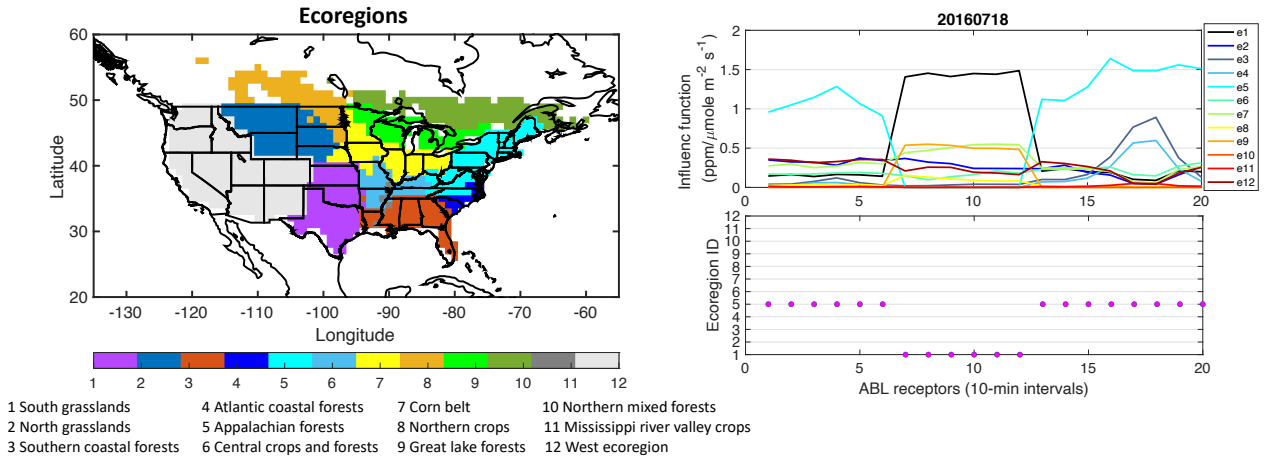

Figure S2. The left panel displays the spatial patterns of ecoregions in Temperate North America defined in the study. The right panel presents an example of this ecoregion tagging process for each receptor in the ABL of one ACT flight.

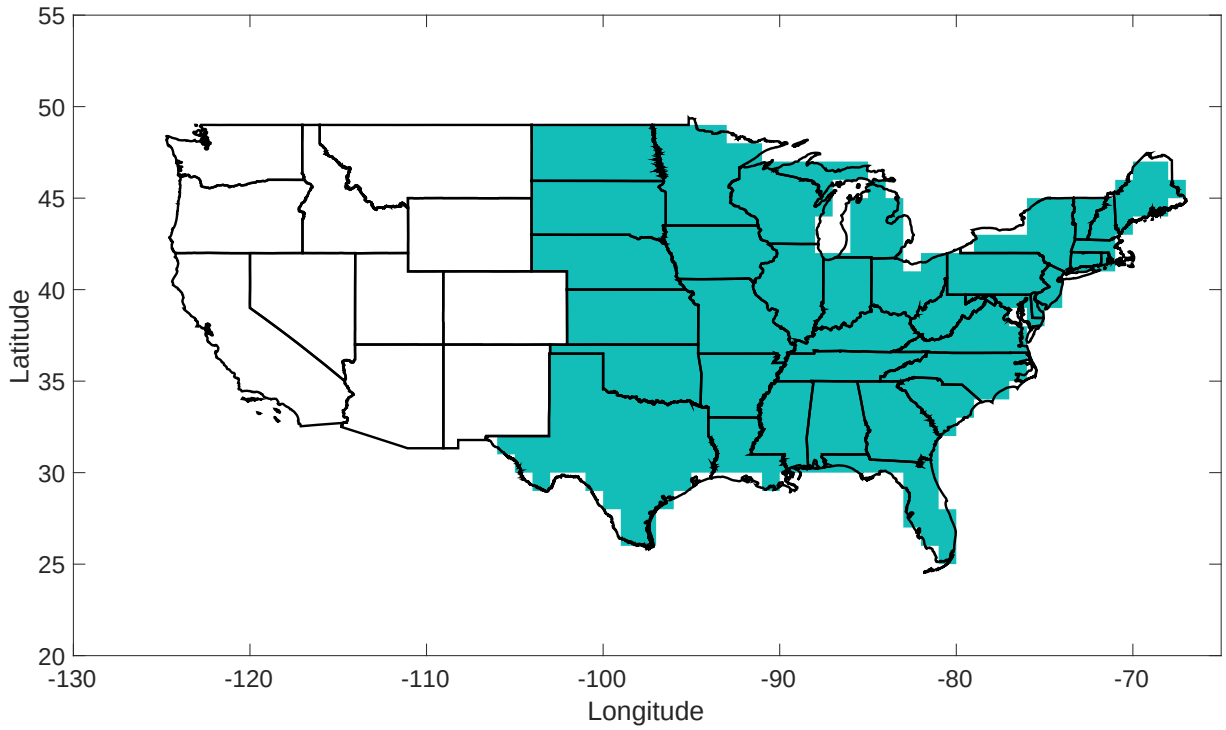

Figure S3. The seasonal NEE flux strength from the shaded areas are calculated for Figure 3.

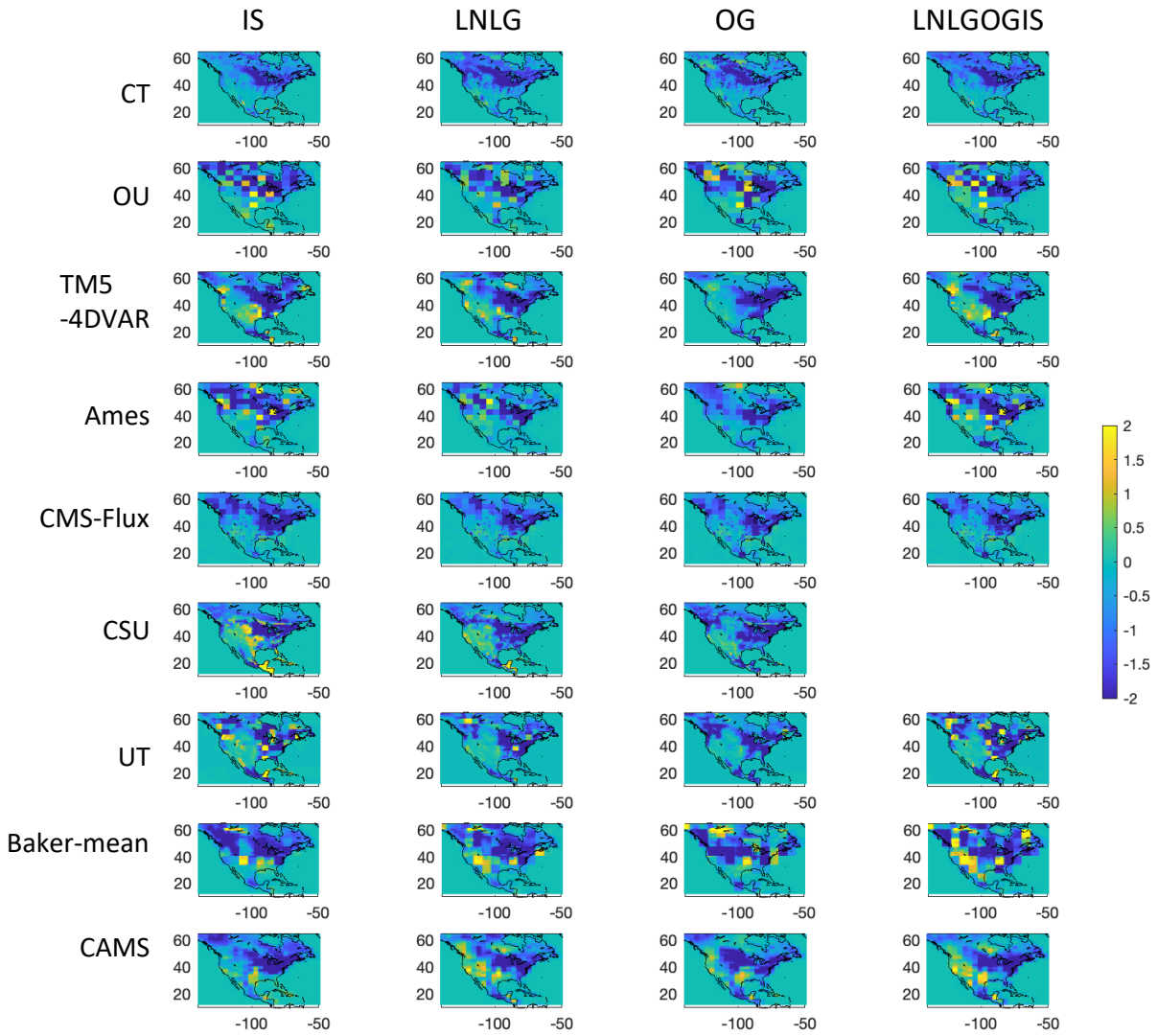

Figure S4. Averaged CO2 NEE fluxes (unit:µmol m-2 s-1) during July-August 2016.

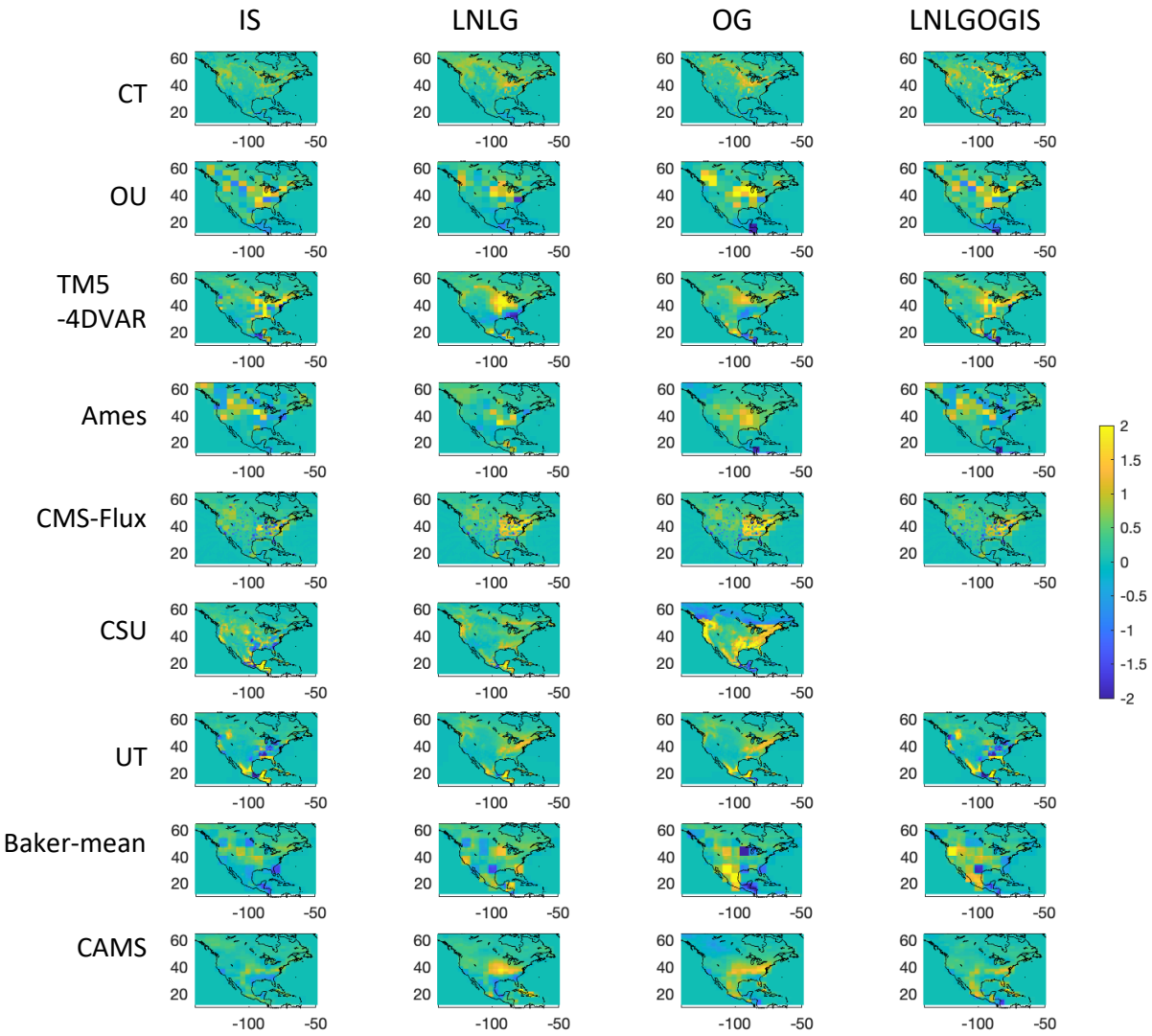

Figure S5. Averaged CO2 NEE fluxes (unit:µmol m-2 s-1) during February-March 2017.

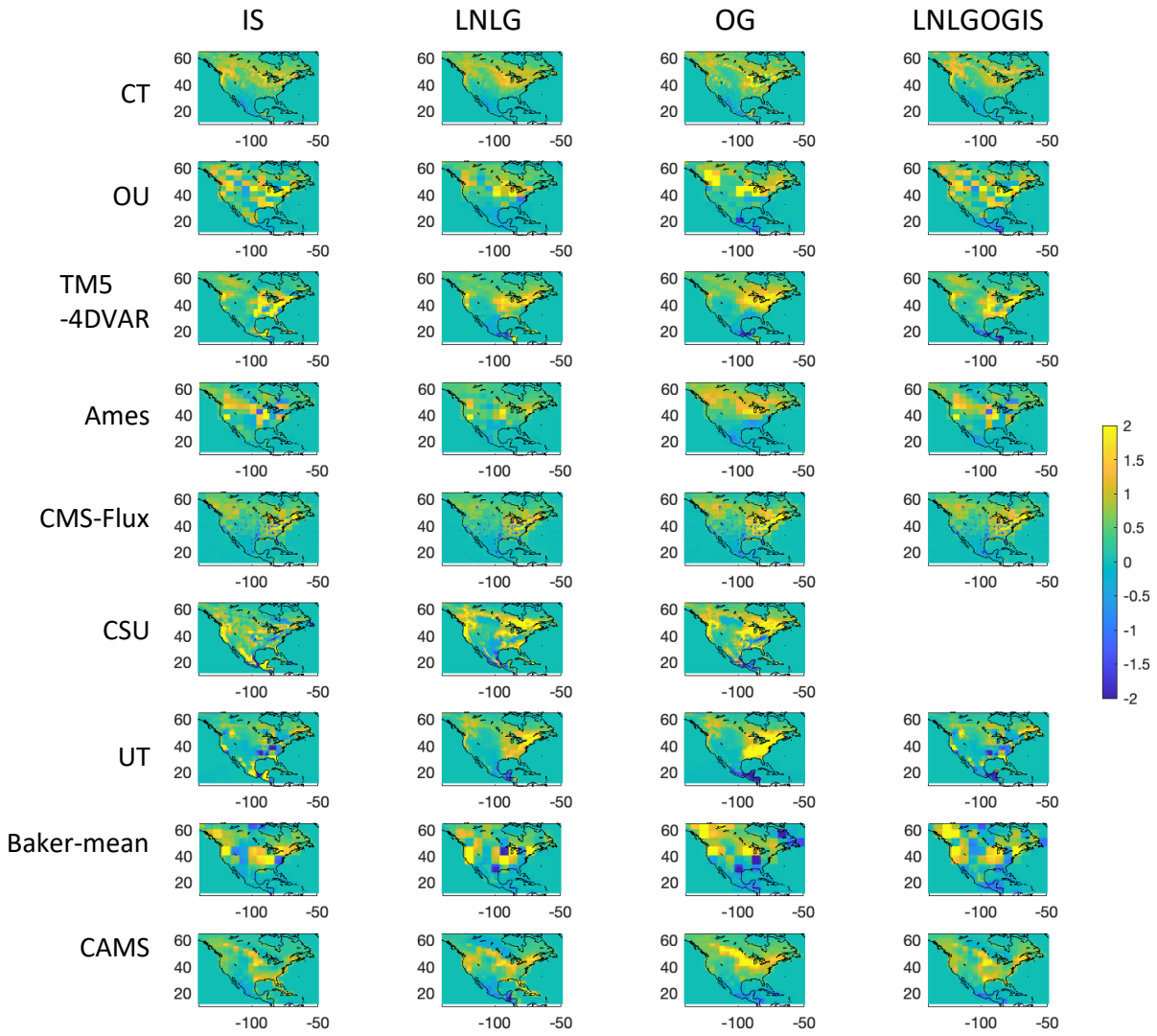

Figure S6. Averaged CO2 NEE fluxes (unit:µmol m-2 s-1) during October-November 2017.

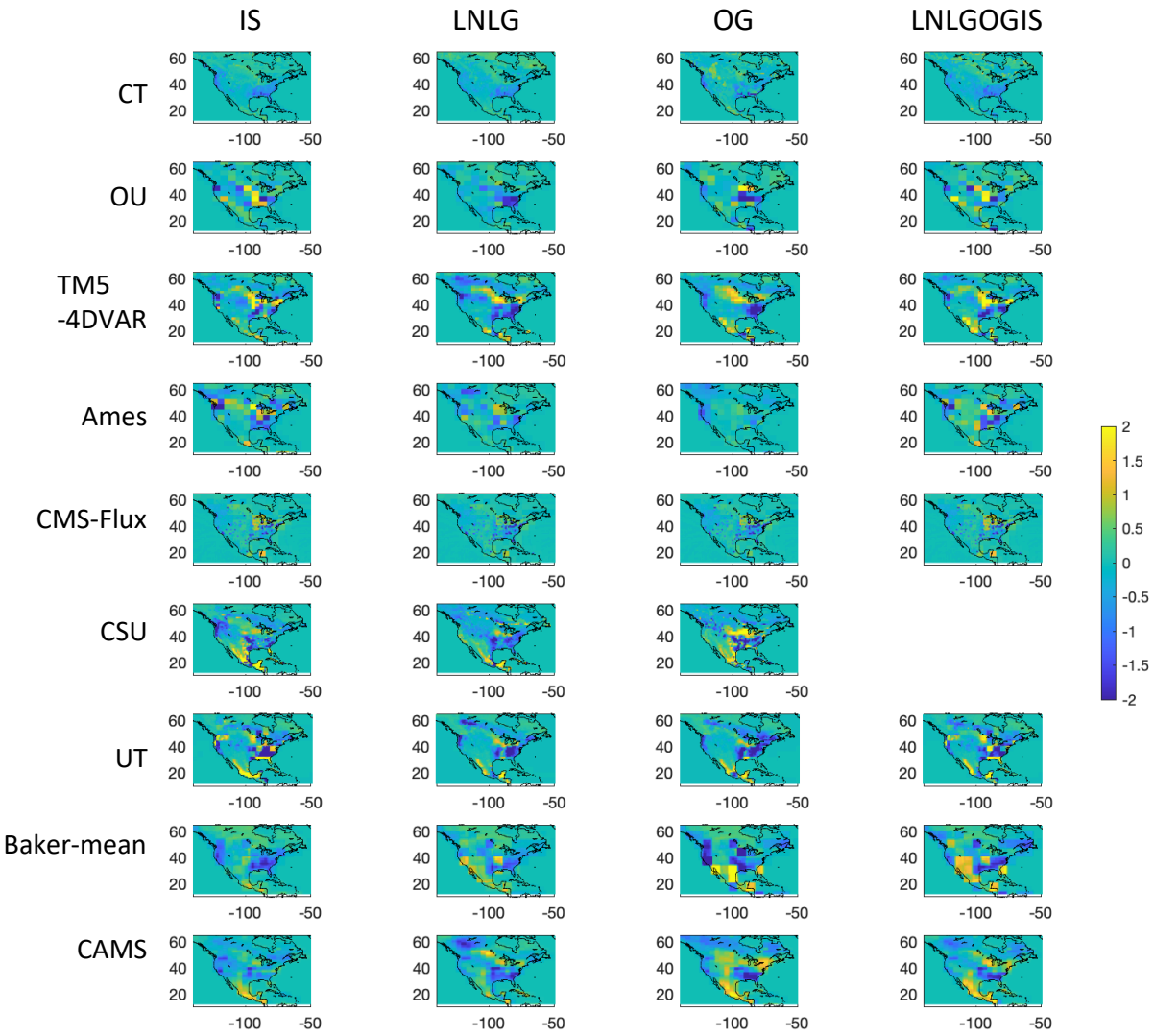

Figure S7. Averaged CO2 NEE fluxes (unit:µmol m-2 s-1) during April-May 2018